Semi-Implicit Roe-Type Fluxes for Low-Mach Number Flows

Jean-Frédéric Gerbeau, Nathalie Glinsky-Olivier, Bernard Larrouturou

INRIA

INSTITUT NATIONAL DE RECHERCHE EN INFORMATIQUE ET EN AUTOMATIQUE

SEMI-IMPLICIT ROE-TYPE FLUXES FOR LOW-MACH NUMBER FLOWS

Jean-Frédéric GERBEAU , Nathalie GLINSKY-OLIVIER and Bernard LARROUTUROU

N° 3132

Mars 1997

THÈME 4

ISSN 0249-6399

INRIA
SOPHIA ANTIPOLIS

SEMI-IMPLICIT ROE-TYPE FLUXES FOR LOW-MACH NUMBER FLOWS

Jean-Frédéric GERBEAU [*], Nathalie GLINSKY-OLIVIER [**] and Bernard LARROUTUROU [***]

Thème 4 — Simulation et optimisation
de systèmes complexes
Projet Caiman

Rapport de recherche n° 3132 — Mars 1997 — 33 pages

Abstract: Two semi-implicit methods based on the splitting of the Euler equations flux into fluid and acoustic parts applied to low Mach number flows are presented. The first method is based on the splitting of slow and fast eigenvalues of the jacobian matrix of the fluxes and a semi-implicit scheme is constructed by introducing only the fast eigenvalues in the implicit matrices. The second method is based on the splitting of the Euler flux by separating the terms in velocity and the terms in pressure ; this system is solved by a fractional step method. A semi-implicit scheme is obtained by using a linearised implicit scheme for the acoustic step only. These two methods are applied to the convection of a density pulse for Mach numbers equal to 0.1 and 0.01. Accuracy and efficiency of the different schemes are compared.

Key-words: Euler equations, low Mach number, semi-implicit scheme, upwind scheme, Roe scheme, finite volume

(Résumé : tsvp)

[*] CERMICS, Marne La Vallée
[**] Projet CAIMAN
[***] INRIA et Ecole Polytechnique, Palaiseau

Unité de recherche INRIA Sophia Antipolis
2004 route des Lucioles, BP 93, 06902 SOPHIA ANTIPOLIS Cedex (France)
Téléphone : 04 93 65 77 77 – Télécopie : 04 93 65 77 65

FLUX DE ROE SEMI-IMPLICITES POUR LES ECOULEMENTS A PETIT NOMBRE DE MACH

Résumé : On présente deux méthodes semi-implicites basées sur la décomposition du flux des équations d'Euler en parties fluide et acoustique pour la résolution d'écoulements à petit nombre de Mach. La première méthode est basée sur la séparation des valeurs propres lentes et rapides de la matrice jacobienne des flux et un schéma semi-implicite est construit en n'incluant que les valeurs propres rapides dans les matrices implicites. La second méthode repose sur une décomposition du flux d'Euler en séparant les termes contenant la vitesse des termes en pression ; cette décomposition est résolue par une approche à pas fractionnaire. On obtient un schéma semi-implicite en appliquant un schéma implicite linéarisé à la seule étape en pression. Ces deux méthodes sont appliquées à la convection d'une vague de densité pour des nombres de Mach égaux à 0.1 et 0.01. On compare la précision et l'efficacité des différents schémas.

Mots-clé : équations d'Euler, petit nombre de Mach, schéma semi-implicite, schéma de Roe, volumes finis

1 Introduction and motivation

We are interested in the numerical simulation of compressible flows at low Mach numbers, such as the ones arising for instance in flame propagation phenomena.

It is well-known that the disparity between the material velocity u and the sound speed c in such flows makes the fully explicit schemes very inefficient. To illustrate this point, assume that the Mach number is $\mathcal{M} = \dfrac{|u|}{c} = 10^{-2}$. Then, an explicit method may operate with the following time step, obtained from the classical CFL condition:

$$\Delta t \approx \Delta t_f = \frac{\Delta x}{|u| + c} \approx \frac{\Delta x}{c} \ . \tag{1.1}$$

We will call this time step Δt_f the "acoustic time step"; the subscript "f" in Δt_f stands for "fast", since the acoustic waves travel much faster than the flow particles. Then, a wave propagating with the velocity u (and this is approximately the case of a flame) will need 100 time steps (i.e., $\mathcal{M}^{-1}$) before it crosses a single spatial cell ! Such an extreme inefficiency is inacceptable in practice for many problems. Ideally, one would like to operate with a time step of the order of the " convective time step", i.e. with:

$$\Delta t \approx \Delta t_s = \frac{\Delta x}{|u|} \ , \tag{1.2}$$

using a fully or partially implicit scheme (the subscript "s" in Δt_s stands for "slow").

Several methods have been proposed these last years in this direction. Most of them rely on the asymptotic analysis of low Mach number flows, which enlights the way in which a compressible flow tends to an incompressible flow as $\mathcal{M}$ approaches 0. These methods therefore have similarities with the methods for incompressible fluid mechanics; in particular they use an implicit solution of an elliptic equation for the pressure (see [7], [8], [12]). Other methods deal with the related difficulties which are met for the simulation of steady low Mach number flows ; since these methods use time-inconsistent preconditioning (see e.g. [1]), they are irrelevant for time-dependent low Mach number flows, which we consider in the present study.

We follow here a different approach initially introduced by G. Fernandez [4]. The goal of this work is to develop a method which remains as close as possible to the methods employed for flows with moderate or even large Mach numbers. More precisely, it introduces a decomposition between "acoustic" and "convective" terms inside the framework of the well-known Roe scheme for the Euler equations, so as to construct a method with the following properties:

> *(i)* The method is conservative, uses Roe-type upwind fluxes, and can stably operate with the convective time step Δt_s ;
>
> *(ii)* The method is "explicit for the convection and implicit for the acoustics". (1.3)

To clarify the condition *(ii)*, "integrating the convection" with an explicit scheme is motivated by accuracy considerations : for the advection equation $\rho_t + u\rho_x = 0$ (with u constant), the first-order accurate upwind explicit scheme operating with $\Delta t \leq \Delta t_s$ is less dissipative than an implicit scheme operating with the same time step (see e.g. [2] and Remark 3.2 below). Besides, we have to "integrate the acoustics" implicitly in order to avoid the acoustic restriction (1.1) on the time step.

Two Roe-type methods aimed at computing low Mach number flows, i.e. satisfying conditions *(i)* and *(ii)*, will be presented and analysed in Sections 3 and 4 below. We will then discuss some numerical results and conclude our work in the last sections.

2 Notations and basic schemes

Let us first introduce some notations and recall some basic facts about the first-order and second-order accurate Roe schemes.

We will consider for the moment only the one-dimensional Euler equations, which we write :

$$W_t + F_x = 0 \ , \tag{2.1}$$

with:

$$W = (\rho, \rho u, E)^T \ , \quad F = \left(\rho u, \rho u^2 + p, u(E+p)\right)^T \ , \tag{2.2}$$

$$p = (\gamma - 1)\left(E - \frac{1}{2}\rho u^2\right) \ . \tag{2.3}$$

The jacobian matrix $A(W) = \dfrac{\partial F}{\partial W}$ being diagonalisable, we may write:

$$A = T\Lambda T^{-1} \ , \tag{2.4}$$

the matrix Λ being diagonal: $\Lambda = \mathrm{Diag}(u-c, u, u+c)$; $c = \sqrt{\dfrac{\gamma p}{\rho}}$ is the sound speed. The columns of the matrix T are the right eigenvectors of A; in particular, we will use below the fact that the eigenvector associated with the second eigenvalue u is proportional to $\left(1, u, \dfrac{u^2}{2}\right)^T$:

$$A(W)\left(1, u, \frac{u^2}{2}\right)^T = u\left(1, u, \frac{u^2}{2}\right)^T \ . \tag{2.5}$$

We will also need the following non-conservative form of (2.1), with the so-called "physical" variables:

$$\tilde{W}_t + \tilde{A}\tilde{W}_x = 0 \ , \tag{2.6}$$

with $\tilde{W} = (\rho, u, p)^T$ and:

$$\tilde{A} = \begin{pmatrix} u & \rho & 0 \\ 0 & u & \rho^{-1} \\ 0 & \gamma p & u \end{pmatrix} \ . \tag{2.7}$$

The first-order explicit Roe scheme writes [9] :

$$\frac{W_j^{n+1} - W_j^n}{\Delta t} + \frac{\phi_{j+1/2}^n - \phi_{j-1/2}^n}{\Delta x} = 0 \ , \tag{2.8}$$

with:

$$\phi_{j+1/2}^n = \Phi\left(W_j^n, W_{j+1}^n\right) = \frac{F(W_j^n) + F(W_{j+1}^n)}{2} + \frac{1}{2}|\hat{A}_{j+1/2}^n|(W_j^n - W_{j+1}^n) \ ; \tag{2.9}$$

here, $\hat{A}_{j+1/2}^n = A(\hat{W}_{j+1/2}^n)$ is the Roe matrix at the interface $j+1/2$, $\hat{W}_{j+1/2}^n$ being the Roe-average of W_j^n and W_{j+1}^n (see e.g. [9]). Let us recall in particular for future use that the Roe-averaged velocity is given by:

$$\hat{u}_{j+1/2}^n = \frac{\sqrt{\rho_j^n}u_j^n + \sqrt{\rho_{j+1}^n}u_{j+1}^n}{\sqrt{\rho_j^n} + \sqrt{\rho_{j+1}^n}} \ . \tag{2.10}$$

A linearized implicit version of this scheme is usually written as [10] :

$$\frac{W_j^{n+1} - W_j^n}{\Delta t} + \frac{\phi_{j+1/2}^{n+1} - \phi_{j-1/2}^{n+1}}{\Delta t} = 0 \ , \tag{2.11}$$

where the flux $\phi_{j+1/2}^{n+1}$, written as an approximate linearization of (2.9), is given by (we denote $\delta W_j = W_j^{n+1} - W_j^n$):

$$\begin{aligned} \phi_{j+1/2}^{n+1} = \ & \frac{F(W_j^n) + F(W_{j+1}^n)}{2} + \frac{1}{2}|\hat{A}_{j+1/2}^n|\left(W_j^n - W_{j+1}^n\right) \\ & + \frac{A(W_j^n)\delta W_j + A(W_{j+1}^n)\delta W_{j+1}}{2} + \frac{1}{2}|\hat{A}_{j+1/2}^n|\left(\delta W_j - \delta W_{j+1}\right) \ . \end{aligned} \tag{2.12}$$

Lastly, we need to introduce a second-order accurate version of the explicit scheme (2.8)-(2.9). We consider the following scheme, introduced by Hancock and Van Leer [11] and extended to finite elements by Fezoui [6], which proceeds in three steps:

$$\frac{\tilde{W}_j^{n+1/2} - \tilde{W}_j^n}{\Delta t/2} + \tilde{A}(\tilde{W}_j^n)s_j^n = 0 \ , \quad \text{with } s_j^n = \frac{\tilde{W}_{j+1} - \tilde{W}_{j-1}}{2\Delta x} \ , \tag{2.13}$$

$$\tilde{W}_{j+1/2,-}^{n+1/2} = \tilde{W}_j^{n+1/2} + \frac{\Delta x}{2}s_j^n \ , \quad \tilde{W}_{j-1/2,+}^{n+1/2} = \tilde{W}_j^{n+1/2} - \frac{\Delta x}{2}s_j^n \ , \tag{2.14}$$

$$\frac{W_j^{n+1} - W_j^n}{\Delta t} + \frac{\Phi\left(W_{j+1/2,-}^{n+1/2}, W_{j+1/2,+}^{n+1/2}\right) - \Phi\left(W_{j-1/2,-}^{n+1/2}, W_{j-1/2,+}^{n+1/2}\right)}{\Delta x} = 0 \ . \tag{2.15}$$

Notice that the predictor and the interpolation steps are written with the physical variables $\tilde{W}$; the predictor is based on the semi-linear form (2.6) of the Euler equations.

3 The acoustic-convective characteristic splitting

Following the idea proposed by G. Fernandez [4], we introduce a first method satisfying our requirements (1.3). This method, called characteristic acoustic-convective splitting, is briefly recalled here. We then will establish some accuracy and stability properties for a simplified problem.

3.1 The first-order acccurate method

Using the diagonalization (2.4) of the jacobian matrix A, we can introduce the two following matrices:

$$A_s = T\Lambda_s T^{-1} \ , \quad A_f = T\Lambda_f T^{-1} \ , \tag{3.1}$$

with:

$$\Lambda_s = \mathrm{Diag}(0, u, 0) \ , \quad \Lambda_f = \mathrm{Diag}(u-c, 0, u+c) \ . \tag{3.2}$$

Thus, we have split the matrix A into a "slow" matrix A_s and a "fast" matrix A_f, according to the characteristic speeds $u-c$, u and $u+c$; obviously we have $A = A_s + A_f$.

We can now introduce the basic, first-order accurate, version of the characteristic acoustic-convective splitting. The method is based on the linearized implicit scheme (2.11)-(2.12), and takes the form:

$$\frac{W_j^{n+1} - W_j^n}{\Delta t} + \frac{\phi_{j+1/2}^{n+1} - \phi_{j-1/2}^{n+1}}{\Delta x} = 0 \ , \tag{3.3}$$

with now (still denoting $\delta W_j = W_j^{n+1} - W_j^n$):

$$\begin{aligned} \phi_{j+1/2}^{n+1} = \quad & \frac{F(W_j^n) + F(W_{j+1}^n)}{2} + \frac{1}{2}|\hat{A}_{j+1/2}^n| \left(W_j^n - W_{j+1}^n\right) \\ & + \frac{A_f(W_j^n)\delta W_j + A_f(W_{j+1}^n)\delta W_{j+1}}{2} + \frac{1}{2}|\hat{A}_{f,j+1/2}^n| \left(\delta W_j - \delta W_{j+1}\right) \ . \end{aligned} \tag{3.4}$$

In words, we keep only the fast part of the matrices in the implicit part, i.e. in the last line of (3.4).

In order to analyse the scheme (3.3)-(3.4), we will first consider its application to a *linear* hyperbolic system. Since the equations for each characteristic variable decouple from each other in such a case, it suffices to consider a 2×2 system. We therefore consider the system:

$$U_t + AU_x = 0 \ , \tag{3.5}$$

where $U = (v, w)^T \in I\!R^2$ and where A is the fixed diagonal matrix:

$$A = \begin{pmatrix} \lambda_s & 0 \\ 0 & \lambda_f \end{pmatrix} \ . \tag{3.6}$$

Assuming that $|\lambda_s| \ll |\lambda_f|$, we will say that v (resp. w) is the slow (resp. fast) variable, and set:

$$A_s = \begin{pmatrix} \lambda_s & 0 \\ 0 & 0 \end{pmatrix} , \quad A_f = \begin{pmatrix} 0 & 0 \\ 0 & \lambda_f \end{pmatrix} . \tag{3.7}$$

For the sake of simplicity, we will assume that λ_s and λ_f are both positive. Setting $F(U) = AU$, we can apply the scheme (3.3)-(3.4) to the linear system (3.5). It is then obvious to prove the following result, which shows that our objectives (1.3) are fulfilled in this linear framework :

LEMMA 3.1:
When applied to the linear system (3.5), *the scheme* (3.3)-(3.4) *reduces to :*

$$\begin{cases} \dfrac{v_j^{n+1} - v_j^n}{\Delta t} + \lambda_s \dfrac{v_j^n - v_{j-1}^n}{\Delta x} = 0 \ , \\ \dfrac{w_j^{n+1} - w_j^n}{\Delta t} + \lambda_f \dfrac{w_j^{n+1} - w_{j-1}^{n+1}}{\Delta x} = 0 \ . \end{cases} \tag{3.8}$$

It is therefore explicit for the slow variable v and implicit for the fast variable w. It is stable under the condition :

$$\frac{\lambda_s \Delta t}{\Delta x} \leq 1 \ , \tag{3.9}$$

which only involves the slow characteristic speed λ_s. •

Now, we would like to turn back to the Euler equations (2.1). Since the analysis of the behaviour of the method (3.3)-(3.4) for the solution of these equations in a general case is out of reach, we will restrict our attention to the following particular (but instructive) situation : we will consider the solution of the Euler equations with an initial data satisfying :

$$u(x, t = 0) \equiv u_0 \ , \quad p(x, t = 0) \equiv p_0 \ , \tag{3.10}$$

where u_0 and p_0 are constant. For the sake of simplicity, we will assume that $u_0 > 0$. It is clear that the Euler equations then reduce to the advection of the density, i.e. that:

$$u(x, t) \equiv u_0 \ , \quad p(x, t) \equiv p_0 \ , \tag{3.11}$$

$$\rho_t(x, t) + u_0 \rho_x(x, t) = 0 \ , \tag{3.12}$$

for all x and t. We can then state:

PROPOSITION 3.2:
When applied to the Euler equations (2.1) *with an initial data satisfying* (3.10), *the explicit scheme* (2.8) *and the semi-implicit scheme* (3.3)-(3.4) *both reduce to:*

$$\begin{cases} u_j^n = u_0 \ , \quad p_j^n = p_0 \quad \textit{for all } j \textit{ and } n \ , \\ \dfrac{\rho_j^{n+1} - \rho_j^n}{\Delta t} + u_0 \dfrac{\rho_j^n - \rho_{j-1}^n}{\Delta x} = 0 \ , \end{cases} \tag{3.13}$$

whereas the implicit scheme (2.11)-(2.12) *reduces to:*

$$\begin{cases} u_j^n = u_0 \ , \quad p_j^n = p_0 \quad \text{for all } j \text{ and } n \ , \\ \dfrac{\rho_j^{n+1} - \rho_j^n}{\Delta t} + u_0 \dfrac{\rho_j^{n+1} - \rho_{j-1}^{n+1}}{\Delta x} = 0 \ . \bullet \end{cases} \tag{3.14}$$

PROOF : We will only consider the case of the semi-implicit method (3.3)-(3.4), the proof being the same for the two other schemes (2.8) and (2.11)-(2.12).

We therefore want to check that the discrete values given by (3.13) satisfy (3.3)-(3.4). For $n \in I\!N$ and for all j, let us assume that:

$$u_j^n = u_j^{n+1} = u_0 \ , \quad p_j^n = p_j^{n+1} = p_0 \ . \tag{3.15}$$

Setting $V_0 = \left(1, u_0, \frac{u_0^2}{2}\right)^T$, we easily see from (2.2)-(2.3) and (3.14) that:

$$W_j^{n+1} - W_j^n = (\rho_j^{n+1} - \rho_j^n) V_0 \ , \quad W_j^n - W_{j+1}^n = (\rho_j^n - \rho_{j+1}^n) V_0 \ , \tag{3.16}$$

for all j. Moreover, for all index j, the Roe-averaged velocity $\hat{u}_{j+1/2}^n$ is obviously equal to u_0 from (2.10). As a consequence, it follows from (2.5) that both differences (3.16) are eigenvectors of the matrices $A(W_j^n)$, $A(W_{j+1}^n)$ and $\hat{A}_{j+1/2}^n = A(\hat{W}_{j+1/2}^n)$. From (3.1)-(3.2), we can therefore write:

$$A_f(W_j^n)\delta W_j = A_f(W_{j+1}^n)\delta W_{j+1}^n = 0 \ , \tag{3.17}$$

$$|\hat{A}_{f,j+1/2}^n|(\delta W_j - \delta W_{j+1}) = 0 \ , \tag{3.18}$$

$$|\hat{A}_{j+1/2}^n|(W_j^n - W_{j+1}^n) = |u_0|(\rho_j^n - \rho_{j+1}^n) V_0 \ . \tag{3.19}$$

Then, (3.3) reduces to:

$$\frac{W_j^{n+1} - W_j^n}{\Delta t} + \frac{F(W_{j+1}^n) - F(W_{j-1}^n)}{2\Delta x} - \frac{|u_0|}{2} V_0 \left(\frac{\rho_{j+1}^n - 2\rho_j^n + \rho_{j-1}^n}{\Delta x} \right) = 0 \ , \tag{3.20}$$

which also writes:

$$\frac{\rho_j^{n+1} - \rho_j^n}{\Delta t} \ V_0 + \frac{\rho_{j+1}^n - \rho_{j-1}^n}{2\Delta x} \ u_0 V_0 - \frac{|u_0|}{2} V_0 \left(\frac{\rho_{j+1}^n - 2\rho_j^n + \rho_{j-1}^n}{\Delta x} \right) = 0 \ , \tag{3.21}$$

which is equivalent to (3.13). •

REMARK 3.1: This result deserves several comments. First, it shows that the semi-implicit method (3.3)-(3.4) is equivallent in the present case to the *explicit* upwind scheme (3.13) for the advection equation (3.12). Also, it is important to realize that Proposition 3.2 says little about the stability of the above schemes : indeed, it just says that, in the present case, the explicit scheme (2.8) and the semi-implicit scheme (3.3)-(3.4) are unstable when the advective scheme (3.13) is unstable, i.e. when $\frac{u_0 \Delta t}{\Delta x} > 1$. But, although the stability of the explicit scheme (2.8) is limited by the acoustic restriction (1.1), we may expect that the semi-implicit scheme (3.3)-(3.4) is stable under the convective condition (1.2), i.e.:

$$\frac{u_0 \Delta t}{\Delta x} \leq 1 \ , \tag{3.22}$$

like the scheme (3.13), since it treats the acoustics implicitly. A hint for this fact (which will be confirmed by the numerical experiments) can be seen by considering a spatially uniform state, as it is usually done in order to introduce the acoustic approximation : then, the linearization of the scheme (3.3)-(3.4) is stable under the condition (3.22) from Lemma 3.1. •

REMARK 3.2: Proposition 3.2 also shows that the semi-implicit scheme (3.3)-(3.4) is more accurate in the present case than both schemes (2.8) and (2.11)-(2.12). First, the method (3.3)-(3.4) is more accurate, for the same time step, than the implicit scheme (2.11)-(2.12), since the dissipative error of the advective scheme (3.14) is proportional to (see e.g. [2]):

$$u_0 \Delta x \left(1 + \frac{u_0 \Delta t}{\Delta x}\right) , \tag{3.23}$$

while the dissipative error of the scheme (3.14) is proportional to:

$$u_0 \Delta x \left(1 - \frac{u_0 \Delta t}{\Delta x}\right) , \tag{3.24}$$

hence lower than (3.23) when (3.22) holds. Moreover, the semi-implicit scheme (3.3)-(3.4) will also be eventually less dissipative than the fully explicit scheme (2.8). They both reduce to (3.13), but the semi-implicit method will operate with $\frac{u_0 \Delta t}{\Delta x} \approx 1$, while the fully explicit scheme (2.8) will operate with $\frac{u_0 \Delta t}{\Delta x} \ll 1$ from (1.1). These observations will be confirmed by our numerical experiments. •

3.2 Extension to second-order accuracy

In this section, we will present our contribution to a second-order accurate semi-implicit scheme ; we will show the good properties of our method and prove that it is a real improvement of the scheme initially proposed by G. Fernandez.

We want to extend the semi-implicit scheme (3.3)-(3.4) to second-order accuracy. In fact, we will extend it so that, using the same words as in (1.3), the scheme becomes "explicit and second-order accurate for the convection, and implicit and first-order accurate for the acoustics", so as to keep the strong dissipative properties of (3.3)-(3.4) for the acoustics. Firstly, we have implemented the extension to second-order accuracy proposed by G. Fernandez [4], [5]. This scheme writes :

$$\frac{\tilde{W}_j^{n+1/2} - \tilde{W}_j^n}{\Delta t/2} + \tilde{A}_s(\tilde{W}_j^n) s_j^n = 0 , \quad \text{with } s_j^n = \frac{\tilde{W}_{j+1} - \tilde{W}_{j-1}}{2\Delta x} , \tag{3.25}$$

$$\tilde{W}_{j+1/2,-}^{n+1/2} = \tilde{W}_j^{n+1/2} + \frac{\Delta x}{2} s_j^n , \quad \tilde{W}_{j-1/2,+}^{n+1/2} = \tilde{W}_j^{n+1/2} - \frac{\Delta x}{2} s_j^n , \tag{3.26}$$

$$\frac{W_j^{n+1} - W_j^n}{\Delta t} + \frac{\phi_{j+1/2}^{n+1} - \phi_{j-1/2}^{n+1}}{\Delta x} = 0 \ , \tag{3.27}$$

where, for instance :

$$\begin{aligned}\phi_{j+1/2}^{n+1} = \ & \frac{F_s(W_{j+1/2,-}^{n+1/2}) + F_s(W_{j+1/2,+}^{n+1/2})}{2} + \frac{1}{2}|\hat{A}_{s,j+1/2}^{n+1/2}| \left(W_{j+1/2,-}^{n+1/2} - W_{j+1/2,+}^{n+1/2}\right) \\ & + \frac{F_f(W_j^n) + F_f(W_{j+1}^n)}{2} + \frac{1}{2}|\hat{A}_{f,j+1/2}^n| \left(W_j^n - W_{j+1}^n\right) \\ & + \frac{A_f(W_j^n)\delta W_j + A_f(W_{j+1}^n)\delta W_{j+1}}{2} + \frac{1}{2}|\hat{A}_{f,j+1/2}^n| \left(\delta W_j - \delta W_{j+1}\right)\end{aligned} \tag{3.28}$$

and

$$F_s(W) = A_s(W)W, \quad F_f(W) = A_f(W)W. \tag{3.29}$$

Using this scheme, we did not obtain satisfactory results as we will see in the numerical results : even using small time steps, we obtain very important spurious oscillations on the numerical solution.

Trying to explain this phenomenon, we can make some remarks.

In order to apply the predictor only to the "slow" part, a fictitious splitting of the flux is introduced $F = F_s + F_f$ in the two first lines of (3.28) while in the first-order accurate scheme, just appear F and the two matrices A_f and A_s. If we look at the two other terms of the two first lines (the matrices), the fluxes are supposed to be such that :

$$\frac{\partial F_s}{\partial W} = A_s(W) \ , \quad \frac{\partial F_f}{\partial W} = A_f(W) \ . \tag{3.30}$$

In fact, the splitting (3.29) do not verify the condition (3.30).

Another remark is that the separate systems $W_t + [A_s(W)W]_x = 0$ and $W_t + [A_f(W)W]_x = 0$ are not hyperbolic, condition which is necessary to write (3.28). Applied to the Euler equations with the initial data (3.10), the scheme do not seem completely second-order accurate for the advection of the density.

We now propose a modification of this scheme and will show the good properties of our second-order accurate extension.

The scheme takes the following form :

$$\frac{\tilde{W}_j^{n+1/2} - \tilde{W}_j^n}{\Delta t/2} + \tilde{A}_s(\tilde{W}_j^n)s_j^n = 0 \ , \quad \text{with } s_j^n = \frac{\tilde{W}_{j+1} - \tilde{W}_{j-1}}{2\Delta x} \ ,$$

$$\tilde{W}_{j+1/2,-}^{n+1/2} = \tilde{W}_j^{n+1/2} + \frac{\Delta x}{2}s_j^n \ , \quad \tilde{W}_{j-1/2,+}^{n+1/2} = \tilde{W}_j^{n+1/2} - \frac{\Delta x}{2}s_j^n \ ,$$

$$\frac{W_j^{n+1} - W_j^n}{\Delta t} + \frac{\phi_{j+1/2}^{n+1} - \phi_{j-1/2}^{n+1}}{\Delta x} = 0 \ ,$$

with a different writting of the numerical flux :

$$\phi^{n+1}_{j+1/2} = \frac{F(W^{n+1/2}_{j+1/2,-}) + F(W^{n+1/2}_{j+1/2,+})}{2} + \frac{1}{2}|\hat{A}^{n+1/2}_{j+1/2}|\left(W^{n+1/2}_{j+1/2,-} - W^{n+1/2}_{j+1/2,+}\right)$$
$$+\frac{A_f(W^{n+1/2}_{j+1/2,-})\delta W_j + A_f(W^{n+1/2}_{j+1/2,+})\delta W_{j+1}}{2} + \frac{1}{2}|\hat{A}^{n+1/2}_{f,j+1/2}|\left(\delta W_j - \delta W_{j+1}\right) . \tag{3.31}$$

Now, the predicted value $W^{n+1/2}$ appears in the "fast" and "slow" parts. No fictive splitting of F is introduced. As in Section 3.1, we will successively analyse the application of this scheme to the linear system (3.5) and to the Euler equations in the purely convective case (3.10). The analogue of Lemma 3.1 reads:

LEMMA 3.3:

When applied to the linear system (3.5)*, the scheme* (3.25)-(3.31) *reduces to:*

$$\begin{cases} \dfrac{v^{n+1/2}_j - v^n_j}{\Delta t/2} + \lambda_s \dfrac{v^n_{j+1} - v^n_{j-1}}{2\Delta x} = 0 , \\ v^{n+1/2}_{j+1/2,-} = v^{n+1/2}_j + \dfrac{\Delta x}{2}\ \dfrac{v^n_{j+1} - v^n_{j-1}}{2\Delta x} , \\ \dfrac{v^{n+1}_j - v^n_j}{\Delta t} + \lambda_s \dfrac{v^{n+1/2}_{j+1/2,-} - v^{n+1/2}_{j-1/2,-}}{\Delta x} = 0 , \end{cases} \tag{3.32}$$

$$\begin{cases} w^n_{j+1/2,-} = w^n_j + \dfrac{\Delta x}{2}\ \dfrac{w^n_{j+1} - w^n_{j-1}}{2\Delta x} , \\ \dfrac{w^{n+1}_j - w^n_j}{\Delta t} + \lambda_f \dfrac{w^n_{j+1/2,-} - w^n_{j-1/2,-}}{\Delta x} + \lambda_f \dfrac{\left(w^{n+1}_j - w^n_j\right) - \left(w^{n+1}_{j-1} - w^n_{j-1}\right)}{\Delta x} = 0 . \end{cases} \tag{3.33}$$

It is explicit second-order accurate for the slow variable v and implicit first-order accurate for the fast variable w. Lastly, it is stable under the condition:

$$\frac{\lambda_s \Delta t}{\Delta x} \leq 1 , \tag{3.34}$$

which only involves the slow characteristic speed λ_s. •

PROOF: Obtaining the relations (3.32)-(3.33) is straightforward. The scheme (3.32) for v is exactly the linear version of the Hancock-Van Leer scheme (2.13)-(2.15); it is known to be second-order accurate and stable under the condition (3.34).

To complete the proof, it remains to show that the (non classical) implicit scheme (3.33) for the variable w is unconditionnally stable. Using a Fourier analysis, we insert $w^n_j = G^n e^{ij\xi}$

for all j and n in (3.33), where G is the amplification factor and ξ the spatial frequency. Setting $\nu = \dfrac{\lambda_f \Delta t}{\Delta x}$, we obtain from (3.33):

$$G - 1 + \nu \left(1 + \frac{e^{i\xi} - e^{-i\xi}}{4}\right) \left(1 - e^{-i\xi}\right) + \nu(G-1)\left(1 - e^{-i\xi}\right) = 0 \ , \tag{3.35}$$

and:

$$G = \frac{1 - \nu \left(1 - e^{-i\xi}\right) \left(\dfrac{e^{i\xi} - e^{-i\xi}}{4}\right)}{1 + \nu \left(1 - e^{-i\xi}\right)}. \tag{3.36}$$

It is then a simple exercice to show that $|G| \leq 1$, for any value of $\nu > 0$. Indeed, the inequality $|G|^2 \leq 1$ is equivallent to:

$$\left|1 - \frac{\nu}{2} \sin\xi \left(i(1 - \cos\xi) - \sin\xi\right)\right|^2 \leq |1 + \nu(1 - \cos\xi) + \nu i \sin\xi|^2 \ . \tag{3.37}$$

Expanding these expressions, substituting $1 - \cos^2\xi$ for $\sin^2\xi$ and setting $X = \cos\xi$, we obtain:

$$\nu(1 + X) + \frac{\nu^2}{2}(1 - X^2) \leq 2\nu + 2\nu^2 \ , \tag{3.38}$$

or equivalently:

$$\frac{\nu^2}{2} X^2 - \nu X + \frac{3\nu^2}{2} + \nu \geq 0 \ . \tag{3.39}$$

Seeing the left-hand side of (3.39) as a second-order polynomial in X, it is easy to show that (3.39) holds for any $\nu > 0$ and $X \in [-1, 1]$. •

We can also state the analogue of Proposition 3.2:

PROPOSITION 3.4:
When applied to the Euler equations (2.1) *with an initial data satisfying* (3.10), *the semi-implicit scheme* (3.25)-(3.31) *reduces to:*

$$u_j^n = u_0 \ , \quad p_j^n = p_0 \quad \text{for all } n \text{ and } j \ , \tag{3.40}$$

$$\begin{cases} \dfrac{\rho_j^{n+1/2} - \rho_j^n}{\Delta t/2} + u_0 \dfrac{\rho_{j+1}^n - \rho_{j-1}^n}{2\Delta x} = 0 \ , \\ \\ \rho_{j+1/2,-}^{n+1/2} = \rho_j^{n+1/2} + \dfrac{\Delta x}{2} \dfrac{\rho_{j+1}^n - \rho_{j-1}^n}{2\Delta x} \ , \\ \\ \dfrac{\rho_j^{n+1} - \rho_j^n}{\Delta t} + u_0 \dfrac{\rho_{j+1/2,-}^{n+1/2} - \rho_{j-1/2,-}^{n+1/2}}{\Delta x} = 0 \ . \bullet \end{cases} \tag{3.41}$$

We omit the proof, which follows exactly the same lines as the proof of Proposition 3.2. The reader should notice that (3.41) is exactly the second-order accurate *explicit* advective scheme (3.32). Our semi-implicit method (3.25)-(3.31) therefore keeps the promising properties of the first-order method (3.3)-(3.4); this will be confirmed by our numerical experiments.

3.3 Numerical results

We present the numerical results obtained for the nonlinear case described above. The calculations have been realised in two dimensions of space for a rectangular domain $[0.;120]\times[0.;30.]$. At initial state, the pressure and the velocity are constant ($\vec{V} = (1.,0.)$), and the density (at $y = 15.$) is presented on figure 1.

We present two solutions for a Mach number equal to 0.1 and 0.01.

As the convection of the initial density profile is an exact solution of the Euler equations, all the numerical solutions will be compared to this exact solution. We also precise that during the different calculations, we control that the pressure and the velocity remain constant equal to the initial value.

The results of the first order accurate explicit, semi-implicit and implicit schemes are compared on figure 2 (resp. 3) for a Mach number equal to 0.1 (resp. 0.01). The behavior of the two cases (Mach number equal to 0.1 and 0.01) is the same. The scheme being first-order accurate in space, the results are not very good but we can notice that the semi-implicit scheme provides the best solutions as it has been proved in remark 3.2.

We now present the solutions obtained with the second-order accurate schemes. Firstly, on figure 4, we present the solution obtained with the extension to second-order accuracy proposed by G. Fernandez. The two results correspond to two values of the time step. The first solution (DT1) has been obtained using the same time step as our version of the second-order accurate scheme (half the time step used for the first-order accurate semi-implicit scheme). It shows a chaotic behavior of the solution. When we employ a smaller time step (DT2, the fifth of the first-order accurate scheme time step) the solution is less oscillating but the maximum value of the density is quite higher than the exact solution. Nevertheless, in both case, the value of the pressure and density remain constant during the calculation ; this is an argument to detail the writing of the scheme instead of thinking to a stability problem.

Secondly, we present, on figure 5 (resp. figure 6), the solutions of the explicit, semi-implicit and implicit second-order accurate schemes for a Mach number equal to 0.1 (resp. 0.01). We notice that the implicit scheme is very diffusive. The solutions of the explicit and the semi-implicit schemes are very good and very close. We can notice a little oscillation around the pulse due to the fact that we do not use any limitor for the extension to the second-order accuracy. Concerning the efficiency of this method, the semi-implicit scheme is nearly 5 times more efficient than the explicit scheme for a flow at Mach=0.1 and more than 40 times better for Mach number equal to 0.01.

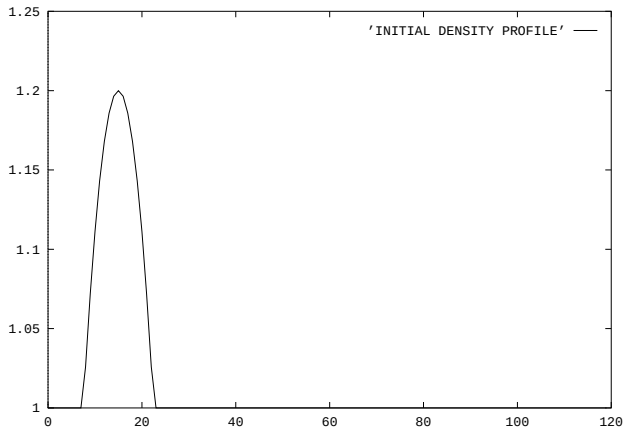

Figure 1: Initial profile of the density at y=15.

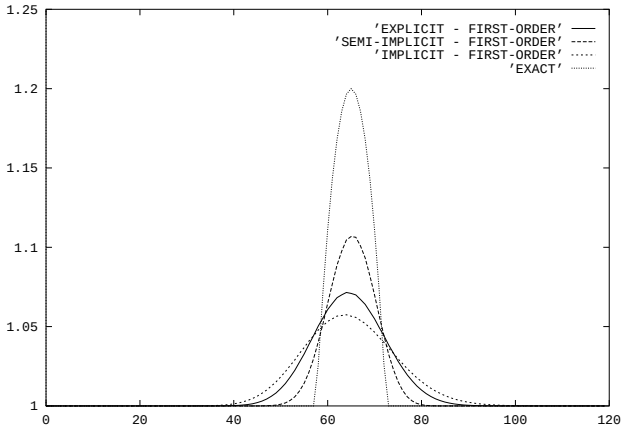

Figure 2: First-order accurate schemes - Mach=0.1

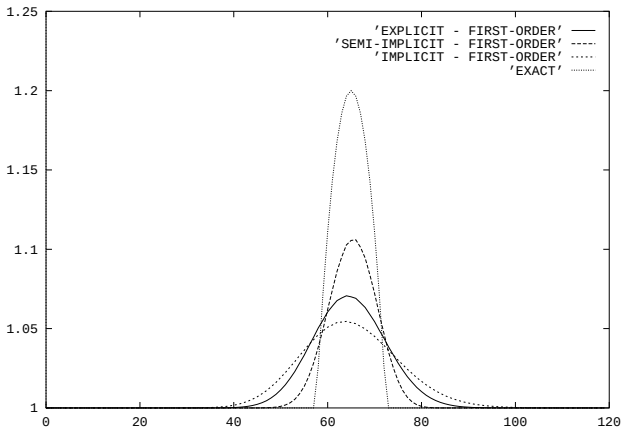

Figure 3: First-order accurate schemes - Mach=0.01

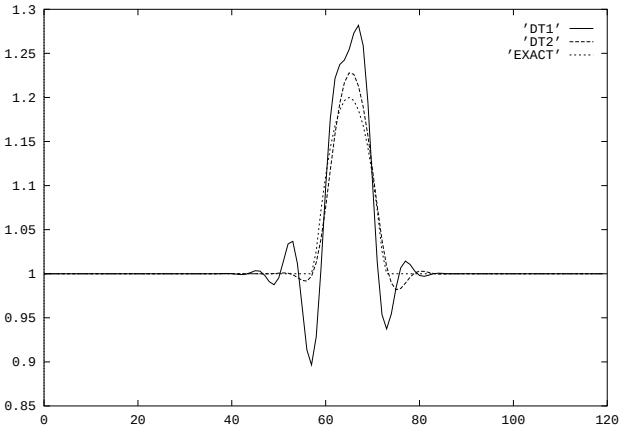

Figure 4: First version of the second-order accurate semi-implicit scheme - Mach=0.01

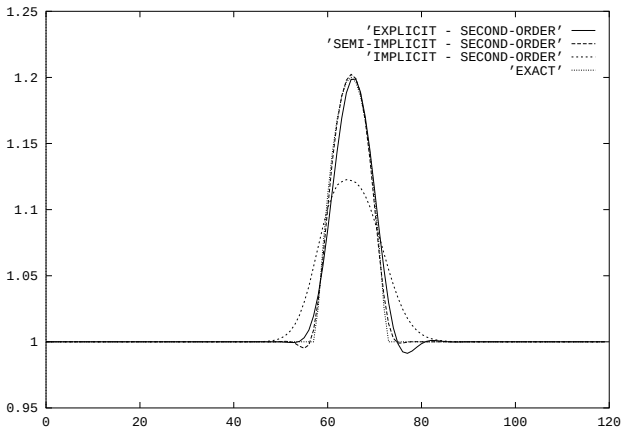

Figure 5: Second-order accurate schemes - Mach=0.1

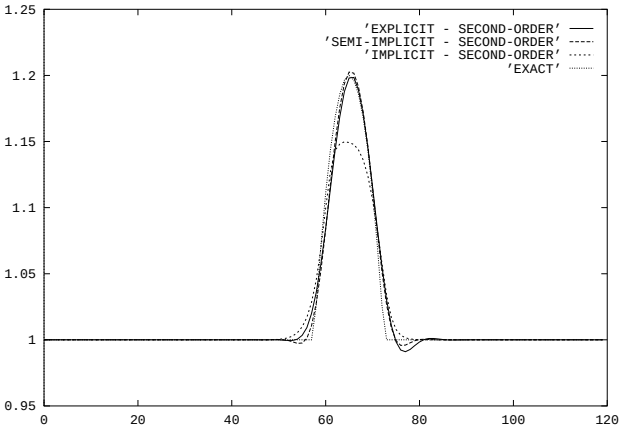

Figure 6: Second-order accurate schemes - Mach=0.01

4 The acoustic-convective flux splitting

After the characteristic acoustic-convective method based on a separation of the eigenvalues of the Jacobian matrix of the flux, we present here another method based on the splitting of the flux into an acoustic and a convective part transforming the initial problem into the solution of two sub-systems. This splitting and the fractional step approach used to solve these two systems have been introduced by T. Buffard [3].

Applying the same idea as in the previous section, which consists in solving explicitly the convection and implicitly the acoustics, we construct a semi-implicit scheme and extend it to second-order accuracy in space.

For simplicity, we present the method in one dimension of space. The one-dimensional Euler equations are written [3] :

$$W_t + F^1(W)_x + F^2(W)_x = 0 \tag{4.1}$$

where

$$F^1(W) = \left(\rho\, u,\ \rho\, u^2,\ u\, E\right)^t \quad \text{and} \quad F^2(W) = (0,\ p,\ u\, p)^t \tag{4.2}$$

The Jacobian matrix

$$A^1(W) = \frac{\partial F^1}{\partial W} = \begin{pmatrix} 0 & 1 & 0 \\ -u^2 & 2u & 0 \\ -u\dfrac{E}{\rho} & \dfrac{E}{\rho} & u \end{pmatrix} \tag{4.3}$$

has the following eigenvalues

$$\lambda_i = u, \quad i = 1, .., 3. \tag{4.4}$$

This matrix is not diagonalizable ; the right eigenvectors span $\mathbb{R}^2$.

The Jacobian matrix

$$A^2(W) = \frac{\partial F^2}{\partial W} = \begin{pmatrix} 0 & 0 & 0 \\ (\gamma-1)\dfrac{u^2}{2} & -(\gamma-1)u & \gamma-1 \\ u\left((\gamma-1)\dfrac{u^2}{2} - \dfrac{p}{\rho}\right) & -(\gamma-1)u^2 + \dfrac{p}{\rho} & (\gamma-1)u \end{pmatrix} \tag{4.5}$$

has the following eigenvalues

$$\lambda_1 = 0,\ \lambda_2 = -c',\ \lambda_3 = c' \ \text{ where } \ c' = \sqrt{\frac{(\gamma-1)\,p}{\rho}} \tag{4.6}$$

The fractional step method writes

$$\underline{\text{Step 1}}\text{:} \quad \text{convection} \qquad W_t + F^1(W)_x = 0$$

$$\underline{\text{Step 2}}\text{:} \quad \text{acoustics} \qquad W_t + F^2(W)_x = 0$$

4.1 The first-order accurate method

Using the same notations as in the previous sections, the first-order explicit fractional step scheme writes :

Step 1

$$\frac{W_j^\star - W_j^n}{\Delta t} + \frac{\phi^1(W_j^n, W_{j+1}^n) - \phi^1(W_{j-1}^n, W_j^n)}{\Delta x} = 0 \tag{4.7}$$

Step 2

$$\frac{W_j^{n+1} - W_j^\star}{\Delta t} + \frac{\phi^2(W_j^\star, W_{j+1}^\star) - \phi^2(W_{j-1}^\star, W_j^\star)}{\Delta x} = 0 \tag{4.8}$$

The numerical flux ϕ^1 is calculated applying the following upwind scheme :

$$\phi^1(W_i, W_j) = \begin{cases} F^1(W_i) & \text{if } \hat{u} > 0 \\ F^1(W_j) & \text{if } \hat{u} < 0 \\ \frac{1}{2}\left(F^1(W_i) + F^1(W_j)\right) & \text{if } \hat{u} = 0 \end{cases} \tag{4.9}$$

where

$$\hat{u} = \frac{\sqrt{\rho_i}\, u_i + \sqrt{\rho_j}\, u_j}{\sqrt{\rho_i} + \sqrt{\rho_j}}$$

and with the additional condition

$$\phi^1(W_i, W_j) = 0 \text{ if } u_i < 0 < u_j. \tag{4.10}$$

More details about the obtention of this scheme can be found in [3].

The second system being hyperbolic, the numerical flux ϕ^2 is calculated using the classical Roe scheme

$$\phi^2(W_i, W_j) = \frac{F^2(W_i) + F^2(W_j)}{2} + \frac{1}{2}|A^2\left(\hat{W}\right)|(W_i - W_j)$$

where the matrix

$$|A^2(W)| = c' \begin{pmatrix} 0 & 0 & 0 \\ -u & 1 & 0 \\ \frac{u^2}{2} & 0 & 1 \end{pmatrix}$$

After calculation, ϕ^2 reduces to

$$\phi^2(W_i, W_j) = \frac{1}{2} \begin{pmatrix} 0 \\ p_i + p_j - \hat{c'}\,\hat{\rho}\,(u_j - u_i) \\ u_i\, p_i + u_j\, p_j - \hat{c'}\,\hat{\rho}\,\hat{u}\,(u_j - u_i) \end{pmatrix} \tag{4.11}$$

where

$$\hat{\rho} = \sqrt{\rho_i\, \rho_j}, \quad \hat{c'} = \sqrt{(\gamma - 1)\left(\frac{\hat{p}}{\rho}\right)} \text{ and } \left(\frac{\hat{p}}{\rho}\right) = \frac{\sqrt{\rho_i}\,\frac{p_i}{\rho_i} + \sqrt{\rho_j}\,\frac{p_j}{\rho_j}}{\sqrt{\rho_i} + \sqrt{\rho_j}} \tag{4.12}$$

To analyse the behavior of this splitting, we will consider, as in the previous sections, the solution of the Euler equations with the initial data satisfying $u\,(x, t=0) \equiv u_0$, $p\,(x, t=0) \equiv p_0$.

PROPOSITION 4.1:
When applied to the Euler equations (4.1) *with an initial data satisfying* (3.10), *the explicit scheme* (4.7)-(4.8) *reduces to:*

$$\left\{ \begin{array}{l} u_j^n = u_0 \ , \quad p_j^n = p_0 \quad \text{for all } j \text{ and } n \ , \\ \\ \dfrac{\rho_j^{n+1} - \rho_j^n}{\Delta t} + u_0 \dfrac{\rho_j^n - \rho_{j-1}^n}{\Delta x} = 0 \ \bullet \end{array} \right. \tag{4.13}$$

PROOF : At $t = n\,\Delta t$, let us assume that for all j, $u_j^n = u_0$ and $p_j^n = p_0$.
Step 1 : Since $\hat{u} = u_0$ and $u_0 > 0$,

$$\phi^1\,(W_i, W_{i+1}) = \left(\begin{array}{c} \rho_i\, u_0 \\ \rho_i\, u_0^2 \\ u_0\, E_i = u_0 \left(\dfrac{\gamma\, p_0}{\gamma - 1} + \dfrac{1}{2}\, \rho_i\, u_0^2 \right) \end{array} \right)$$

The scheme becomes

$$\frac{1}{\Delta t} \left(\begin{array}{c} \rho_i^\star - \rho_i^n \\ (\rho\, u)_i^\star - \rho_i\, u_0 \\ E_i^\star - E_i^n \end{array} \right) + \left(\begin{array}{c} u_0 \\ u_0^2 \\ \dfrac{u_0^3}{2} \end{array} \right) \frac{\rho_i^n - \rho_{i-1}^n}{\Delta x} = 0$$

Since $E = \dfrac{\gamma\, p}{\gamma - 1} + \dfrac{1}{2}\, \rho\, u^2$, we easily show that the first step reduces to

$$\left\{ \begin{array}{l} \dfrac{\rho_i^\star - \rho_i^n}{\Delta t} + u_0\, \dfrac{\rho_i^n - \rho_{i-1}^n}{\Delta x} = 0 \\ u_i^\star = u_0, \quad p_i^\star = p_0 \end{array} \right.$$

Step 2 : Since for all j, $u_j^\star = u_0$, the Roe scheme writes very simply

$$\phi^2\,(W_i, W_j) = \left(\begin{array}{c} 0 \\ p_0 \\ u_0\, p_0 \end{array} \right)$$

Then, the second step becomes

$$W_i^{n+1} - W_i^\star = 0$$

and the demonstration of the proposition is achieved.

We can write a semi-implicit version of the fractional step scheme by applying a linearized implicit scheme for the acoustic step. This scheme writes :

Step 1

$$\frac{W_j^\star - W_j^n}{\Delta t} + \frac{\phi^1\left(W_j^n, W_{j+1}^n\right) - \phi^1\left(W_{j-1}^n, W_j^n\right)}{\Delta x} = 0 \tag{4.14}$$

Step 2

$$\frac{W_j^{n+1} - W_j^\star}{\Delta t} + \frac{\phi^2\left(W_j^{n+1}, W_{j+1}^{n+1}\right) - \phi^2\left(W_{j-1}^{n+1}, W_j^{n+1}\right)}{\Delta x} = 0 \tag{4.15}$$

where

$$\begin{aligned}\phi^2\left(W_j^{n+1}, W_{j+1}^{n+1}\right) = \quad & \frac{F^2\left(W_j^\star\right) + F^2\left(W_{j+1}^\star\right)}{2} + \frac{1}{2}|A^2\left(\tilde{W}\right)|\left(W_j^\star - W_{j+1}^\star\right) \\ & + \frac{A^2\left(W_j^\star\right)\,\delta W_j + A^2\left(W_{j+1}^\star\right)\,\delta W_{j+1}}{2} + \frac{1}{2}|A^2\left(\hat{W}\right)|\left(\delta W_j - \delta W_{j+1}\right)\end{aligned} \tag{4.16}$$

where $\delta W_j = W_j^{n+1} - W_j^\star$.

We can also write an implicit version of the fractional step where the convective and the acoustic step are treated implicitly. The scheme writes :

Step 1

$$\frac{W_j^\star - W_j^n}{\Delta t} + \frac{\phi^1\left(W_j^\star, W_{j+1}^\star\right) - \phi^1\left(W_{j-1}^\star, W_j^\star\right)}{\Delta x} = 0 \tag{4.17}$$

Step 2

$$\frac{W_j^{n+1} - W_j^\star}{\Delta t} + \frac{\phi^2\left(W_j^{n+1}, W_{j+1}^{n+1}\right) - \phi^2\left(W_{j-1}^{n+1}, W_j^{n+1}\right)}{\Delta x} = 0 \tag{4.18}$$

where the linearization of the convective numerical flux expresses as :

$$\phi^1\left(W_j^\star, W_{j+1}^\star\right) = \phi^1\left(W_j^n, W_{j+1}^n\right) + \frac{\partial \phi^1\left(W_j^n\right)}{\partial W}\left(W_j^\star - W_j^n\right) + \frac{\partial \phi^1\left(W_{j+1}^n\right)}{\partial W}\left(W_{j+1}^\star - W_j^n\right) \tag{4.19}$$

where

$$\frac{\partial \phi^1\left(W_j^n\right)}{\partial W} = \begin{cases} \dfrac{\partial F^1}{\partial W}\left(W_j\right) & \text{if } \hat{u} > 0 \\ 0 & \text{if } \hat{u} < 0 \\ \dfrac{1}{2}\dfrac{\partial F^1}{\partial W}\left(W_j\right) & \text{if } \hat{u} = 0 \end{cases} \quad \text{and} \quad \frac{\partial \phi^1\left(W_{j+1}^n\right)}{\partial W} = \begin{cases} 0 & \text{if } \hat{u} > 0 \\ \dfrac{\partial F^1}{\partial W}\left(W_{j+1}\right) & \text{if } \hat{u} < 0 \\ \dfrac{1}{2}\dfrac{\partial F^1}{\partial W}\left(W_{j+1}\right) & \text{if } \hat{u} = 0 \end{cases} \tag{4.20}$$

4.2 Extension to the second-order accuracy

To extend the scheme to second-order spatial accuracy, we employ the same method as already described for the acoustic-convective characteristic splitting. For instance, for the explicit version of the method, we apply a predictor-corrector scheme at each step. The scheme writes :

Step 1

$$\left\{ \begin{array}{l} \dfrac{\tilde{W}_j^{n+1/2} - \tilde{W}_j^n}{\Delta t/2} + \tilde{A}^1\left(\tilde{W}_j^n\right) s_j^n = 0 \ \text{ with } \ s_j^n = \dfrac{\tilde{W}_{j+1}^n - \tilde{W}_{j-1}^n}{2\,\Delta x} \\ \tilde{W}_{j+1/2,-}^{n+1/2} = \tilde{W}_j^{n+1/2} + \dfrac{\Delta x}{2} s_j^n, \ \ \tilde{W}_{j-1/2,+}^{n+1/2} = \tilde{W}_j^{n+1/2} - \dfrac{\Delta x}{2} s_j^n \\ \dfrac{W_j^\star - W_j^n}{\Delta t} + \dfrac{\phi^1\left(W_{j+1/2,-}^{n+1/2}, W_{j+1/2,+}^{n+1/2}\right) - \phi^1\left(W_{j-1/2,-}^{n+1/2}, W_{j-1/2,+}^{n+1/2}\right)}{\Delta x} = 0 \end{array} \right. \tag{4.21}$$

Step 2

$$\left\{ \begin{array}{l} \dfrac{\tilde{W}_j^{\star\star} - \tilde{W}_j^\star}{\Delta t/2} + \tilde{A}^2\left(\tilde{W}_j^\star\right) s_j^\star = 0 \ \text{ with } \ s_j^\star = \dfrac{\tilde{W}_{j+1}^\star - \tilde{W}_{j-1}^\star}{2\,\Delta x} \\ \tilde{W}_{j+1/2,-}^{\star\star} = \tilde{W}_j^{\star\star} + \dfrac{\Delta x}{2} s_j^\star, \ \ \tilde{W}_{j-1/2,+}^{\star\star} = \tilde{W}_j^{\star\star} - \dfrac{\Delta x}{2} s_j^\star \\ \dfrac{W_j^{n+1} - W_j^\star}{\Delta t} + \dfrac{\phi^2\left(W_{j+1/2,-}^{\star\star}, W_{j+1/2,+}^{\star\star}\right) - \phi^2\left(W_{j-1/2,-}^{\star\star}, W_{j-1/2,+}^{\star\star}\right)}{\Delta x} = 0 \end{array} \right. \tag{4.22}$$

where $\tilde{A}^1$ and $\tilde{A}^2$ are the matrices coming from the non-conservative form and $\tilde{W}$ is the physical variable. The expression of the matrices is the following ;

$$\tilde{A}^1 = \begin{pmatrix} u & \rho & 0 \\ 0 & u & 0 \\ 0 & p & u \end{pmatrix} \qquad \tilde{A}^2 = \begin{pmatrix} 0 & 0 & 0 \\ 0 & 0 & \rho^{-1} \\ 0 & (\gamma-1)\,p & 0 \end{pmatrix}$$

and we verify that $\tilde{A}^1 + \tilde{A}^2 = \tilde{A}$.

We can also write a semi-implicit version of the second-order accurate scheme by mixing a predictor-corrector second-order accurate scheme for the first step and an implicit second-order accurate scheme for the second step. The expression of the scheme is

Step 1 : same expression as (4.21).

Step 2

$$\left\{ \begin{array}{l} \tilde{W}_{j+1/2,-}^\star = \tilde{W}_j^\star + \dfrac{\Delta x}{2} s_j^\star, \ \ \tilde{W}_{j-1/2,+}^\star = \tilde{W}_j^\star - \dfrac{\Delta x}{2} s_j^\star \\ \qquad \text{with } \ s_j^\star = \dfrac{\tilde{W}_{j+1}^\star - \tilde{W}_{j-1}^\star}{2\,\Delta x} \\ \dfrac{W_j^{n+1} - W_j^\star}{\Delta t} + \dfrac{\phi^2\left(W_{j+1/2,-}^{n+1}, W_{j+1/2,+}^{n+1}\right) - \phi^2\left(W_{j-1/2,-}^{n+1}, W_{j-1/2,+}^{n+1}\right)}{\Delta x} = 0 \end{array} \right. \tag{4.23}$$

the expression of $\phi^2(W^{n+1}_{j+1/2,-}, W^{n+1}_{j+1/2,+})$ being deduced from the linearized implicit scheme (4.16).

We have also implemented an implicit version by introducing the MUSCL approach at both steps without prediction. Step 1

$$\left\{ \begin{array}{l} \dfrac{\tilde{W}_j^{n+1/2} - \tilde{W}_j^n}{\Delta t/2} + \tilde{A}^1\left(\tilde{W}_j^n\right) s_j^n = 0 \ \text{ with } \ s_j^n = \dfrac{\tilde{W}_{j+1}^n - \tilde{W}_{j-1}^n}{2\,\Delta x} \\ \tilde{W}^{n+1/2}_{j+1/2,-} = \tilde{W}_j^{n+1/2} + \dfrac{\Delta x}{2}\, s_j^n, \ \ \tilde{W}^{n+1/2}_{j-1/2,+} = \tilde{W}_j^{n+1/2} - \dfrac{\Delta x}{2}\, s_j^n \\ \dfrac{W_j^\star - W_j^n}{\Delta t} + \dfrac{\phi^1\left(W^{n+1}_{j+1/2,-}, W^{n+1}_{j+1/2,+}\right) - \phi^1\left(W^{n+1}_{j-1/2,-}, W^{n+1}_{j-1/2,+}\right)}{\Delta x} = 0 \end{array} \right. \tag{4.24}$$

where the writing of $\phi^1(W^{n+1}_{j+1/2,-}, W^{n+1}_{j+1/2,+})$ is deduced from the linearized implicit scheme (4.19)-(4.20).
Step 2 : same scheme as (4.23).

4.3 Numerical results

For this scheme, we study the same case as in the previous section i.e. the convection of the density profile presented on figure 1. The conditions are exactly the same as previously: the calculations are done in two dimensions of space, solutions have been obtained for two different values of the Mach number (Mach number = 0.1 and 0.01) and are compared to the exact solution.

The results of the first-order accurate explicit, semi-implicit and implicit schemes are compared on figure 7 (resp. 8) for a Mach number equal to 0.1 (resp. 0.01). We notice that for a Mach number equat to 0.1 the semi-implicit scheme provides the best solution and the implicit scheme is very diffusive. For a Mach number equal to 0.01, no visible difference appear between the solutions of the different schemes. When we compare this solution to the figure 7, we notice that the three solutions are comparable to the result of the explicit scheme. To explain this phenomenon, it firstly seems that the semi-implicit scheme becomes less accurate when the Mach number decreases and secondly, the stability of the implicit scheme do not allow very large time steps ; that can explain the weak diffusion of the implicit scheme in this case.

The results of the second-order accurate explicit, semi-implicit and implicit schemes are presented on figure 9 (resp. 10) for a Mach number equal to 0.1 (resp. 0.01). As for the first-order accurate schemes, the behavior of the solutions depends on the Mach number. For a Mach number equal to 0.1, we remark that the semi-implicit scheme provides the more accurate solutions, better than the explicit scheme and that the accuracy has been really improved. In return, for a Mach number equal to 0.01, we notice that the semi-implicit scheme looses accuracy and provides a solution comparable to that of the explicit scheme. Moreover, the explicit and the semi-implicit schemes produce better solutions than the implicit scheme ; it was not the case for the first-order accurate implicit scheme. Concerning

the efficiency of the second-order accurate schemes, for a Mach number equal to 0.1, the semi-implicit scheme is 50% more efficient than the explicit scheme. On the other hand, for a Mach number equal to 0.01, the gain obtained by using the semi-implicit scheme is about 5% only. The implicit scheme, inverting two matrices at each time step is not efficient compared to the two other schemes, that for both Mach numbers. This result is due to the fact that for stability reasons, it has not been possible to use large time steps in the semi-implicit and implicit schemes.

To show that the accuracy of the semi-implicit scheme is very dependent of the Mach number of the flow, we have realized calculations for Mach numbers equal to 0.025, 0.05, 0.075, 0.11 and 0.125 and we have plotted, on figure 11, the maximum value of the density of the pulse as a function of the Mach number. It is obvious to see that, for the highest values of the Mach number (0.1, 0.11 and 0.125) the accuracy of the scheme is very good and that for lower values of the Mach number, this simple treatment of the equations do not allow accurate solutions.

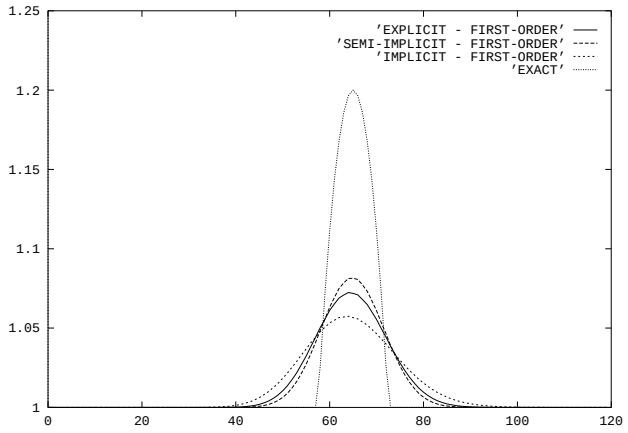

Figure 7: Comparison of first-order schemes - Mach number = 0.1

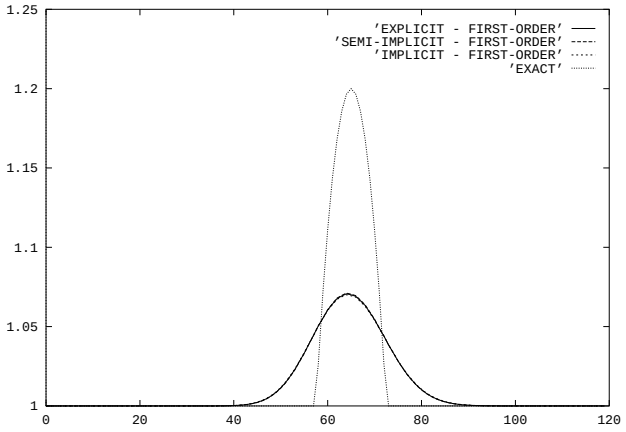

Figure 8: Comparison of first-order schemes - Mach number = 0.01

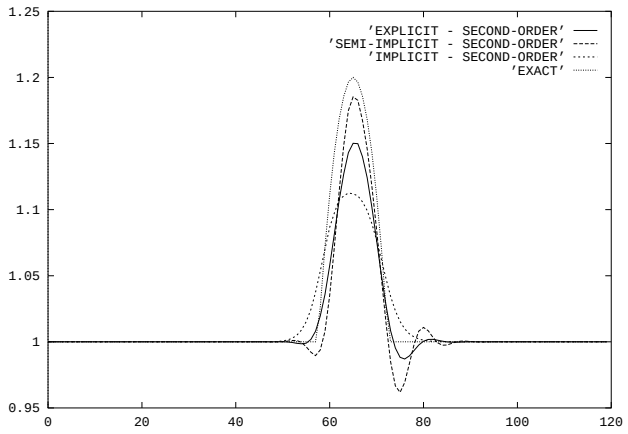

Figure 9: Comparison of second-order schemes - Mach number = 0.1

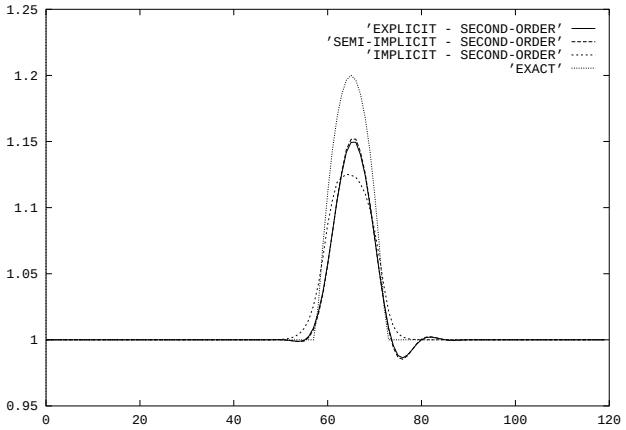

Figure 10: Comparison of second-order schemes - Mach number = 0.01

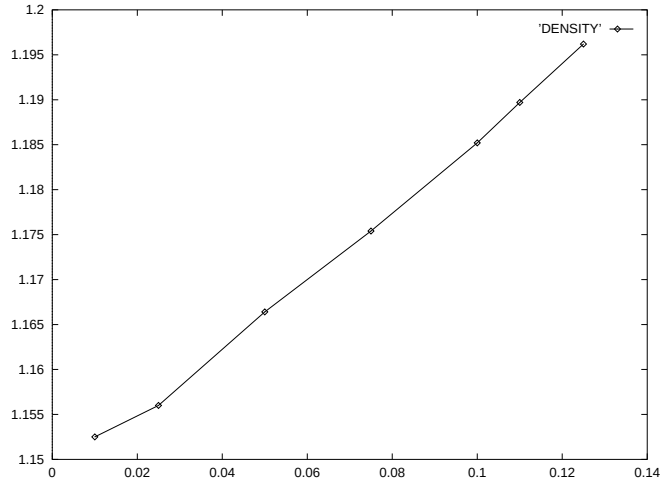

Figure 11: Maximum of the density as function of the Mach number

5 Conclusion

We have presented two different methods to solve low Mach number flow problems.

The first method, called characteristic splitting, is based on a separation of the convective and acoustic eigenvalues in the jacobian matrix of the flux appearing in the Euler equations. The second-order accurate semi-implicit scheme fulfil all the conditions : the solution can be nearly surimposed to the exact solution and the time step allowed by the scheme is almost independent of the Mach number.

The second method, called flux splitting, separates the flux of the Euler equations in a convective and an acoustic part and treats them differently in a fractional step approach. The results obtained for a Mach number equal to 0.1 are encouraging, even if the characteristic splitting method provides better solutions. But, when the Mach number decreases, the accuracy and the efficiency of this method is far from the results of the first method. We could consider an improvement of this method by a more sophisticated treatment of the fractional step approach especially for the second-order accuracy in space ; in practice, for instance for the explicit scheme, we have simply combined two steps of a predictor-corrector scheme without a detailed study of the accuracy and stability properties. This study is the first perspective to this work.

References

[1] Boretti A. An explicit Runge-Kutta method for turbulent reactive flow calculations. In A. Dervieux and B. Larrouturou, editors, *Numerical combustion, Lecture notes in physics*, volume 351. Springer-Verlag, Heidelberg, 1989.

[2] D.A. Anderson, J.C. Tannehill, and R.H. Pletcher. *Computational fluid mechanics and heat transfer.* Hemisphere, Mc Graw Hill, 1984.

[3] T. Buffard. *Analyse de quelques méthodes de Volumes Finis non structurés pour la résolution des équations d'Euler.* PhD thesis, université de Paris VI, décembre 1993.

[4] G. Fernandez. *Simulation numérique d'écoulements réactifs à petit nombre de Mach.* PhD thesis, université de Nice, juin 1989.

[5] G. Fernandez and H. Guillard. A numerical method for the computation of low Mach number reactive flows. In C. Taylor, P. Gresho, R.L. Sani, and J. Hauser, editors, *Proceedings of the 6th Int. Conf. on Numerical methods in laminar and turbulent flows.* Pineridge Press, Swansea, 11-15 july 1989.

[6] F. Fezoui. Résolution des équations d'Euler par un schéma de van Leer en éléments finis. *Research report INRIA*, 358, 1985.

[7] R. Klein. Semi-Implicit Extension of a Godunov-Type Scheme Based on Low Mach Number Asymptotics I: One-Dimensional Flow. *J. Comput. Phys.*, 121:213–237, 1995.

[8] G. Patnaik, R.H. Guirguis, J.P. Boris, and E.S. Oran. A barely implicit correction for the flux-corrected transport. *J. of Comput. Phys.*, 71:1–20, 1987.

[9] P. L. Roe. Approximate Riemann solvers, parameter vectors and difference schemes. *J.C.P.*, 43:357, 1981.

[10] B. Stoufflet. *Résolution numérique des équations d'Euler des fluides parfaits compressibles par des schémas implicites en éléments finis.* PhD thesis, université de Paris VI, mars 1984.

[11] B. van Leer. Computational methods for ideal compressible flows. In *Von Karman Institute, Lecture series*, 1983.

[12] O.C. Zienkiewicz, J. Smeler, and J. Peraire. Compressible and incompressible flow ; an algorithm for all seasons. *Comp. Meth. Appl. Meth. Eng.*, 78:105–121, 1990.

Unité de recherche INRIA Lorraine, Technopôle de Nancy-Brabois, Campus scientifique,
615 rue du Jardin Botanique, BP 101, 54600 VILLERS LÈS NANCY
Unité de recherche INRIA Rennes, Irisa, Campus universitaire de Beaulieu, 35042 RENNES Cedex
Unité de recherche INRIA Rhône-Alpes, 655, avenue de l'Europe, 38330 MONTBONNOT ST MARTIN
Unité de recherche INRIA Rocquencourt, Domaine de Voluceau, Rocquencourt, BP 105, 78153 LE CHESNAY Cedex
Unité de recherche INRIA Sophia Antipolis, 2004 route des Lucioles, BP 93, 06902 SOPHIA ANTIPOLIS Cedex

Éditeur
INRIA, Domaine de Voluceau, Rocquencourt, BP 105, 78153 LE CHESNAY Cedex (France)
ISSN 0249-6399